Topography-Based Surface Tension Gradients to Facilitate Water Droplet Movement on Laser-Etched Copper Substrates

A. D. Sommers,*,[†] T. J. Brest,[‡] and K. F. Eid[‡]

[†]Department of Mechanical and Manufacturing Engineering, Miami University, 56 Garland Hall, Oxford, Ohio 45056, United States
[‡]Department of Physics, Miami University, 35 Culler Hall, Oxford, Ohio 45056, United States

S Supporting Information

ABSTRACT: This paper describes a method for creating a topography-based gradient on a metallic surface to help mitigate problems associated with condensate retention. The gradient was designed to promote water droplet migration toward a specified region on the surface which would serve as the primary conduit for drainage using only the roughness of the surface to facilitate the movement of the droplets. In this work, parallel microchannels having a fixed land width but variable spacing were etched into copper substrates to create a surface tension gradient along the surface of the copper. The surfaces were fabricated using a 355 nm Nd:YVO4 laser system and then characterized using spray testing techniques and water droplet (2−10 μL) injection via microsyringe. The distances that individual droplets traveled on the gradient surface were also measured using a goniometer and CCD camera and were found to be between 0.5 and 1.5 mm for surfaces in a horizontal orientation. Droplet movement was spontaneous and did not require the use of chemical coatings. The theoretical design and construction of surface tension gradients were also explored in this work by calculating the minimum gradient needed for droplet movement on a horizontal surface using Wenzel's model of wetting. The results of this study suggest that microstructural patterning could be used to help reduce condensate retention on metallic fins such as those used in heat exchangers in heating, ventilation, air-conditioning, and refrigeration (HVAC&R) applications.
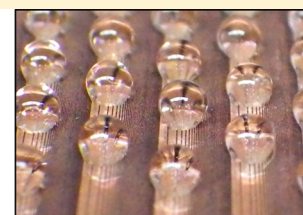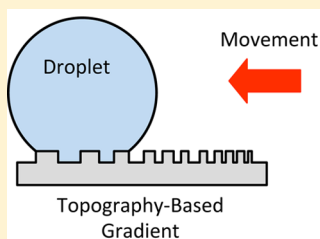
INTRODUCTION

Heat exchangers are important to the overall efficiency, cost, and compactness of many thermal management systems including solar heating applications and heating, ventilation, air-conditioning, and refrigeration (HVAC&R) systems. According to a recent Department of Energy study, the heating, cooling, and lighting of residential and commercial buildings accounted for approximately 18% of the United States' total energy consumption in 2009.[1] Naturally then, increasing the efficiency of the heat exchangers used in these systems is extremely desirable because of the tremendous potential for cost savings and reduction in pollution. Current heat exchanger designs, however, make extensive use of copper and aluminum which are naturally hydrophilic. Because of this intrinsic property, water condenses and adheres to these surfaces in the form of water droplets when the system is operating below the dew point temperature. Once a condensate droplet forms on the surface, it continues to grow and coalesce with other droplets until gravitational, capillary, or air-flow forces are able to remove it. This retention of condensate is often problematic because it can reduce the overall thermal performance of the unit by occupying heat transfer surface area and increasing the core pressure drop. In addition, the retained condensate provides a site for biological activity which may cause odors and can adversely affect human comfort if it is blown off the heat exchanger and carried downstream into the occupied space. Therefore, it is important to understand how

condensate is retained on the heat-transfer surface and how surface tension gradients might assist in facilitating its drainage and removal.

The most common approach to reducing water retention is the use of chemical coatings to decrease the wettability of the surface. While this would certainly increase water drainage on these surfaces, a homogenously coated surface would also permit (even facilitate) condensate carryover into the occupied space. In HVAC&R applications, controlling the direction of condensate movement on the surface is often as important as the physical removal of those droplets. Therefore, a surface with a patterned anisotropic wettability may be preferred since droplet motion can be restricted to one direction—namely, downward with gravity. For example, previous work by Sommers and Jacobi[2] demonstrated that aluminum surfaces with anisotropic microscale topographical features can be used to manipulate the critical droplet size and affect the overall wettability. Furthermore, if a gradient exists on the surface, then a net surface tension force is produced that tries to move the droplet in the direction of the gradient. This could then be used to help move water droplets to a desired location on the fin surface. Adding both the effects of an anisotropic wettability and a surface tension gradient could lead to a significant

reduction in the overall retention of water on heat exchangers used in HVAC&R systems.

One of the earliest works involving surface tension gradients was by Chaudhury and Whitesides who were able to induce the upward motion of small water drops ($1-2$ μL) on surfaces containing a gradient tilted from the horizontal plane by $15°$.[3] The surface energy gradient was created on silicon using a diffusion-controlled process adapted from ref 4 involving silane vapor. Low contact angle hysteresis ($\leq 10°$) was reported as a necessary condition for droplet motion. Daniel et al. later observed the movement of water droplets on a surface with a radial surface tension gradient in which droplets displayed velocities of $0.15-1.5$ m/s.[5] The authors reported that this increase in velocity (over earlier studies) was due to the coalescence of droplets and suggested that this had implications for enhancing heat transfer in heat exchangers. In Daniel and Chaudhury, velocities in the range of $1-2$ mm/s were measured and found to scale nearly linearly with the droplet radius.[6] In each case, chemical modification of the surface was both needed and used in creating the gradient. Shastry et al. described a rough superhydrophobic surface (produced in silicon) with a contact angle gradient accomplished by varying the dimensions and spacing of square micropillars over a distance of 4 to 8 mm.[7] Droplets were propelled down these gradients by mechanical vibration using energy supplied by a speaker. Based on these findings, the surface contact area fraction φ was suggested as a control variable for droplet manipulation. These findings also suggest that wettability gradients (based solely in topographical variation) might be used to facilitate drainage and/or control condensate distribution on the surface prior to the start of frost growth. Several other recent publications (refs 8–23) have been published on the topic.

While the study and application of surface tension gradients is relatively new, most published studies have involved ideal surfaces such as silicon and almost all have been chemistry-based. Furthermore, relatively few papers have documented the application of surface tension gradients on metallic substrates such as aluminum and copper. Moreover, the authors are not aware of any paper that has sought to specifically use topographical modification alone (without the aid of chemical coatings) to create a surface tension gradient capable of controlling water droplet motion. It is important to note that, in the systems motivating this work, chemical coatings tend to break down over time due to the thermal cycling and large temperature gradients experienced in these systems. Thus, the goal of this work was to create a surface tension gradient that was capable of moving small water droplets on a metallic substrate using only the systematic variation of the underlying surface topography. The engineering value of this research rests in both its robustness and its direct application in dehumidification and air-cooling systems for the control of condensate on heat transfer surfaces.

Figure 1. Schematic of a droplet on a (a) homogeneous surface and (b) a surface with an underlying gradient.

■ BACKGROUND AND EXPERIMENTAL METHODOLOGY

The objective of this research was to use the natural anisotropy of a microgrooved surface to create a robust surface tension gradient for water droplet movement by systematically varying the width of the grooves. Water droplet behavior on these surfaces was then studied using a Ramé-Hart goniometer and a charge coupled device (CCD) camera to record droplet travel distance. In the following sections, the minimum gradient force needed for droplet motion is discussed as well as the surface fabrication procedure and experimental setup.

Surface Tension Modeling. If we take a water droplet on a horizontal surface, the net surface tension force along any direction is zero. However, if we create a surface tension gradient, then the contributions from the opposite ends of the droplet (i.e., along the gradient direction) will not completely cancel out. This results in a net surface-tension-gradient force that tries to move the droplet in the direction of the gradient (i.e., in the x-direction). Perhaps more importantly, this surface-tension-gradient force could be used to potentially facilitate the removal of small droplets from a surface and/or droplet movement on a flat horizontal surface.

So how strong of a gradient would be needed to move a droplet on a horizontal surface? To begin, let us consider a simple circular droplet that is deformed due to the existence of an underlying gradient. If the gradient was not present, this droplet would exist as a spherical cap as shown in Figure 1. Now let us consider a simple case where the local contact angle of a droplet on a horizontal surface does vary from one end of the droplet to the other due to the presence of a gradient (see Figure 2) such that

$$\cos \theta(x) = a_1 x^3 + a_2 x^2 + a_3 x + a_4 \tag{1}$$

where

$$\cos \theta(0) = \cos \theta_{max} \tag{2a}$$

$$\cos \theta(D) = \cos \theta_{min} \tag{2b}$$

$$\left. \frac{d(\cos \theta)}{dx} \right|_{x=0} = \psi \tag{2c}$$

$$\left. \frac{d(\cos \theta)}{dx} \right|_{x=D} = \psi \tag{2d}$$

(Note: Eqs 2c and 2d assume a linear gradient with a constant rate of change.) Using these boundary conditions to solve for the constants (i.e., a_1, a_2, a_3, a_4), one finds that

$$\cos \theta(x) = -\frac{2}{D^3}[(\cos \theta_{min} - \cos \theta_{max}) - \psi D]x^3$$
$$+ \frac{3}{D^2}[(\cos \theta_{min} - \cos \theta_{max}) - \psi D]x^2 + \psi x$$
$$+ \cos \theta_{max} \tag{3}$$

The surface tension force associated with this droplet deformation can be calculated using the equation:

$$F_s = -\gamma D \int_0^\pi \cos \theta \cos \phi \, d\phi \tag{4}$$

$$F_s = -\gamma D \int_0^\pi (a_1 x^3 + a_2 x^2 + a_3 x + a_4) \cos \phi \, d\phi \tag{5}$$

Substituting $x = R(1 - \cos \phi)$ into this expression and integrating yields

$$F_s = -\gamma D \left[\frac{-15\pi}{8} a_1 \left(\frac{D}{2}\right)^3 - \pi a_2 \left(\frac{D}{2}\right)^2 - \frac{\pi}{2} a_3 \left(\frac{D}{2}\right) \right] \tag{6}$$
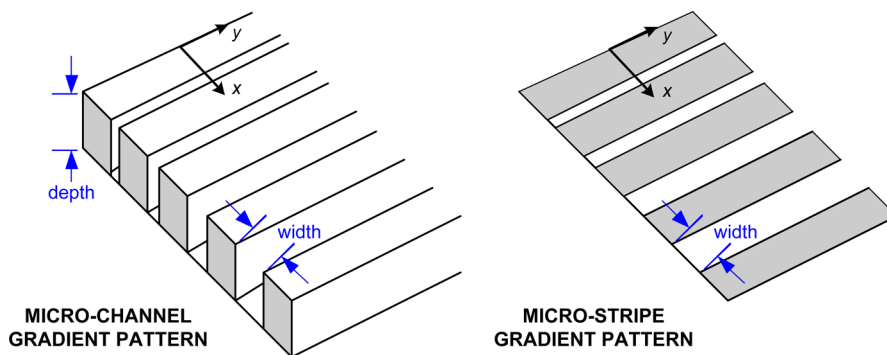
Figure 2. Two possible linear surface tension gradient designs (single gradient pattern shown). In the double gradient design (not shown), both widths are systematically varied.

$$F_s = \gamma D \left[\frac{9\pi}{32} (\cos\theta_{min} - \cos\theta_{max}) - \frac{\pi D}{32}\psi \right] \quad (7)$$

If the variation of the contact angle is linear, then $\psi = (\cos\theta_{min} - \cos\theta_{max})/D$. In this case, the surface tension force equation simplifies to

$$F_s = \frac{8\pi}{32}\gamma D [\cos\theta_{min} - \cos\theta_{max}] \quad (8)$$

So how does this compare to published expressions for the surface tension force on a surface? According to El Sherbini,[24] the surface tension force on a homogeneous surface can be represented as

$$F_s^* = \frac{24}{\pi^3}\gamma D [\cos\theta_{rec} - \cos\theta_{adv}] \quad (9)$$

In the case where the droplet is moving (i.e., $\theta_{max} = \theta_{adv}$ and $\theta_{min} = \theta_{rec}$), then these two expressions yield nearly the same value. Moreover, the leading coefficient in these expressions (referred to as the retentive force factor, k) depends on the shape of the droplet base contour as well as the variation of the contact angle. Various values for k have been suggested.[25−27] This simple analysis, however, shows that, for a droplet to move on a flat surface, it must be able to overcome the contact angle hysteresis (i.e., $\theta_{adv} - \theta_{rec}$).

Design of a Topography-Based Surface Tension Gradient. If the goal of the gradient is to facilitate the movement and growth of water droplets on a metallic surface during condensation, then Wenzel's model of wetting (which can be applied when $\theta < 90°$) is probably the most appropriate for describing the water droplet behavior.[28] In Wenzel's model, the new apparent contact angle θ^* is related to the original contact angle θ through a roughness factor r such that

$$\cos\theta^* = r\cos\theta \quad (10)$$

where r is the area fraction of the liquid/solid contact (i.e., wetted area over the projected area) as shown in Figure 3. (Note: In this model, $r \geq 1$.)

Now, let us consider a small circular droplet sitting atop a horizontal surface patterned with a surface wettability gradient and assume that half of the droplet is characterized by the contact angle θ_1 and half of
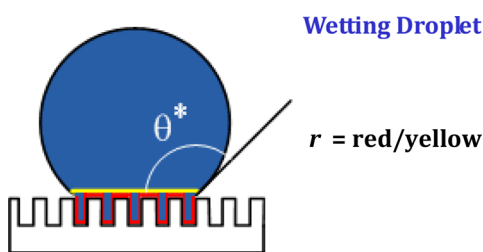
Figure 3. Schematic illustrating the application of Wenzel's model to a wetting droplet.

the droplet is characterized by the angle θ_2 to simplify the analysis (see Figure 4). This approach has been used by others including Dimitrakopoulos and Higdon.[29] Using Wenzel's model then to predict the new contact angles (i.e., θ_1^* and θ_1^*), we can write the surface tension force on a microstructured (or, microstriped) gradient surface as

$$F_s = \gamma D \int_0^{\pi/2} r\cos\theta_1\cos\phi \, d\phi + \gamma D \int_{\pi/2}^{\pi} r\cos\theta_2\cos\phi \, d\phi \quad (11)$$

Let us further assume that the surface tension gradient varies linearly such that

$$r = r_o + \frac{dr}{dx}x = r_o + \frac{dr}{dx}R(1 - \cos\phi) \quad (12a)$$

where

$$r = r_o \quad \text{for} \quad \phi = 0° \quad (12b)$$

$$r = r_o + \frac{dr}{dx}2R \quad \text{for} \quad \phi = 180° \quad (12c)$$

Substituting and simplifying,

$$F_s = 2\gamma R\cos\theta_1\left[r_o + \frac{dr}{dx}R\left(1 - \frac{\pi}{4}\right)\right] - \pi\gamma R^2\cos\theta_2\frac{dr}{dx} - 2\gamma R\cos\theta_2\left[r_o + \frac{dr}{dx}R\left(1 - \frac{\pi}{4}\right)\right] \quad (13)$$

Here, if $F_s \neq 0$, then the droplet should move on the horizontal surface. Therefore, the minimum surface tension gradient necessary for droplet movement on a flat surface is found by setting F_s equal to zero and solving for dr/dx which results in

$$\frac{dr}{dx} = \frac{r_o(\cos\theta_1 - \cos\theta_2)}{R\left[\left(1 + \frac{\pi}{4}\right)\cos\theta_2 - \left(1 - \frac{\pi}{4}\right)\cos\theta_1\right]} \quad (14)$$

If the droplet is moving, then the expression can be rewritten as

$$\frac{dr}{dx} = \frac{r_o(\cos\theta_{rec} - \cos\theta_{adv})}{R\left[\left(1 + \frac{\pi}{4}\right)\cos\theta_{adv} - \left(1 - \frac{\pi}{4}\right)\cos\theta_{rec}\right]} \quad (15)$$

where θ_{adv} and θ_{rec} are the advancing and receding contact angles of the surface, respectively. (Note: The advancing and receding contact angles are key measurements that characterize the hydrophobicity/hydrophilicity of a surface.[30−33]) A few observations can be gleaned from this expression. First, the surface tension gradient necessary for droplet movement on a flat surface scales directly with the contact angle hysteresis. In other words, the larger the underlying hysteresis is, the larger the gradient needs to be to overcome it. Second, the gradient is proportional to the initial roughness factor, r_o. Larger gradients are needed in cases of large initial roughness factors. Third,
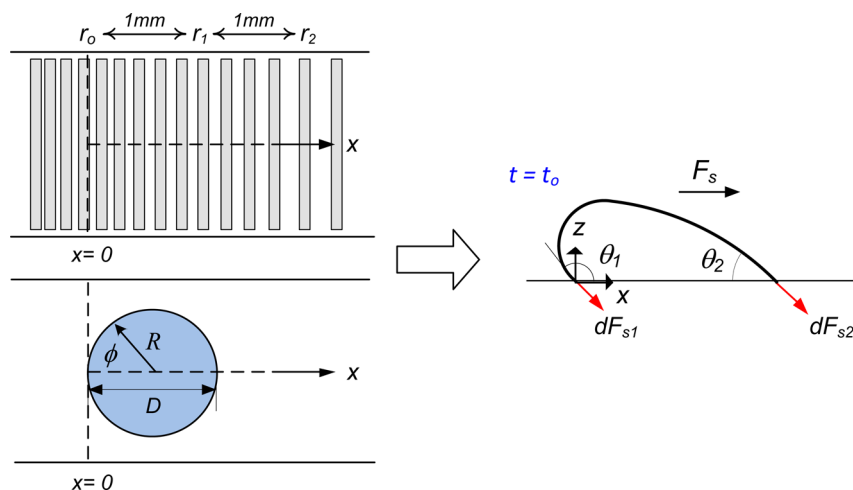
Figure 4. Possible contact angle variation due to an underlying surface tension gradient where the Wenzel roughness parameter, r, is varied in a prescribed manner across the surface.
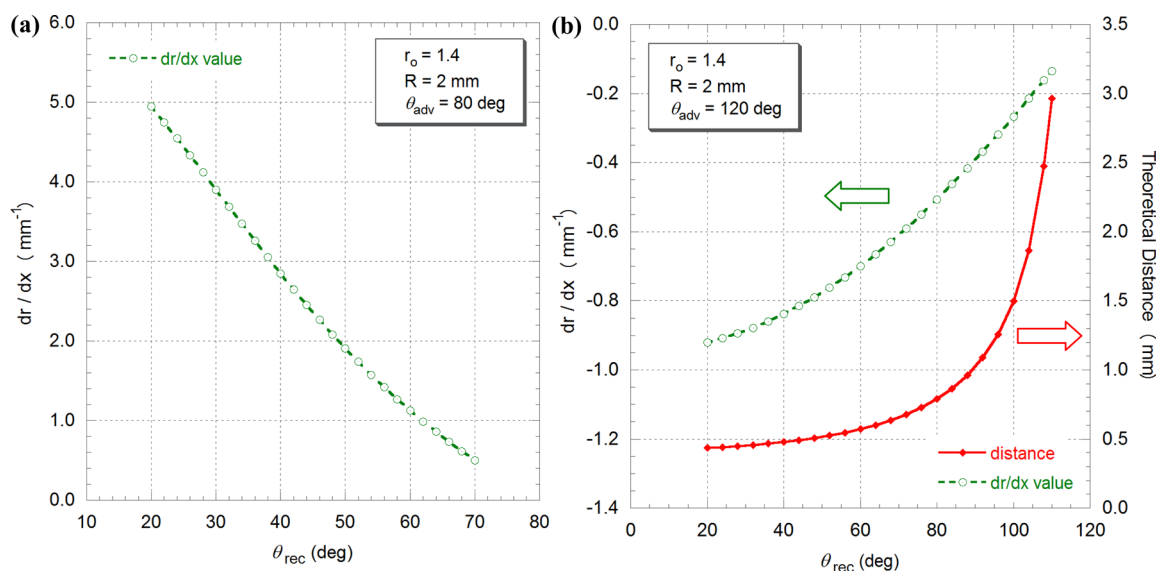
Figure 5. (a) Hydrophilic surface (i.e., $\theta_{adv} < 90°$). Required gradient values, dr/dx, necessary for spontaneous droplet motion on a horizontal surface for $R = 2$ mm and $r_o = 1.4$. (b) Hydrophobic surface (i.e., $\theta_{adv} > 90°$). Required gradient values, dr/dx, necessary for spontaneous droplet motion on a horizontal surface for $R = 2$ mm and $r_o = 1.4$.

Table 1. Calculated Surface Tension Gradient Values, dr/dx, for $r_o = 1.4$ and $R = 2$ mm (units: mm^{-1})

	θ_{rec}										
θ_{adv}	20°	30°	40°	50°	60°	70°	80°	90°	100°	110°	120°
80°	4.949	3.904	2.848	1.909	1.127	0.498	0				
120°	−0.921	−0.887	−0.838	−0.776	−0.700	−0.610	−0.507	−0.392	−0.267	−0.135	0

the surface tension gradient is inversely proportional to the droplet radius, R. This is because as the droplet radius increases, there is more distance for the contact angle to change. Thus, the necessary rate of change of the roughness factor (and hence the surface tension gradient) gets smaller as the droplet size gets larger. Finally, the gradient is smaller on surfaces with large advancing contact angles and larger on surfaces with small receding contact angles. In other words, droplets are more likely to move on surfaces with large advancing angles, whereas droplets are less likely to move on surfaces having small receding contact angles as shown in Table 1.

In Table 1, the gradient values, dr/dx, necessary for spontaneous droplet motion on a horizontal surface are calculated for a droplet radius of 2 mm and an initial surface roughness parameter $r_o = 1.4$. It is important to note that if the underlying surface is naturally wetting (i.e., $\theta < 90°$), positive dr/dx values are calculated. This is because capillarity is the primary mechanism for droplet motion which requires increasing r values (i.e., deeper channels) for the increased wicking of the fluid. In principle, r could be increased indefinitely; however, manufacturing practices would likely limit the maximum depth of the channels. Furthermore, as liquid begins to fill the channels during droplet travel, there would be less and less liquid available for the filling of subsequent channels. According to this model, for $\theta_{adv} = 80°$, $\theta_{rec} = 20°$ (i.e., large hysteresis), and $r_o = 1.4$, the rate of change of the roughness parameter required for droplet motion (i.e., dr/dx) is 4.95 mm^{-1} as shown in Figure 5a; whereas for $\theta_{adv} = 80°$ and $\theta_{rec} = 70°$ (i.e., small hysteresis), the required rate of change of the roughness parameter is only 0.50 mm^{-1}. In other words, when the hysteresis force is small, the surface tension gradient can be more gradual.
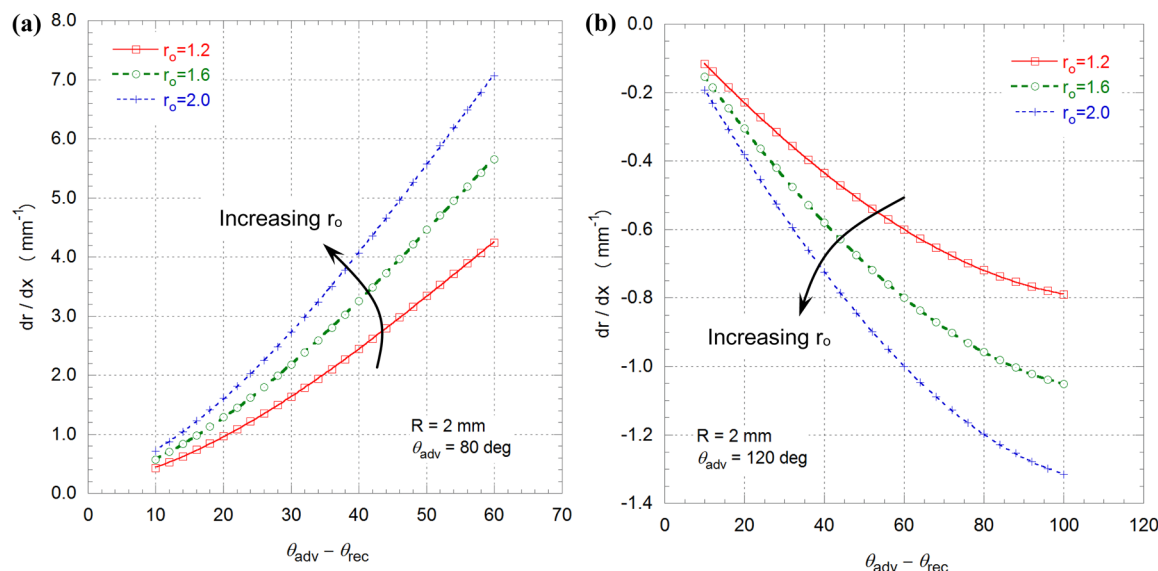
Figure 6. (a) Effect of the initial surface roughness parameter on the dr/dx value for (a) a hydrophilic surface and (b) a hydrophobic surface.

If the underlying surface is naturally nonwetting (i.e., $\theta > 90°$), then negative dr/dx values are calculated. This is because in order for nonwetting droplets to move from regions of high hydrophobicity to regions of increasing hydrophilicity, the r value must be decreasing. In this case, however, there is a natural, self-occurring limit to the design of such gradient surfaces. The value of r can only be decreased down to unity (i.e., smooth surface without any channels). For example, for $R = 2$ mm and $r_o = 1.4$ with $\theta_{adv} = 120°$ and $\theta_{rec} = 20°$ (i.e., large hysteresis), the droplet travel distance is theoretically limited to 0.435 mm; whereas for $\theta_{adv} = 120°$ and $\theta_{rec} = 110°$ (i.e., small hysteresis), the theoretical distance that the droplet should travel increases to 2.96 mm as shown below in Figure 5b. As might be expected, the surface hydrophobicity has a large effect on the predicted travel distance. If the advancing and receding contact angles are increased to $\theta_{adv} = 150°$ and $\theta_{rec} = 140°$ (i.e., same hysteresis) while holding all other parameters constant (i.e., $R = 2$ mm and $r_o = 1.4$), then the theoretical droplet travel distance increases to 7.90 mm, an increase of more than 4.9 mm.

Figure 6 illustrates how the required gradient values, dr/dx, change with the initial roughness of the surface and the contact angle hysteresis. For hydrophilic surfaces, Figure 6a shows the required rate of change of the gradient for spontaneous droplet motion on a surface where $R = 2$ mm and $\theta_{adv} = 80°$. This figure shows that the dr/dx value increases with both increasing r_o (i.e., increased initial roughness) and increasing contact angle hysteresis (i.e., $\theta_{adv} - \theta_{rec}$). Of these two parameters, the effect of the contact angle hysteresis is the most pronounced. (That is, for surfaces with a large contact angle hysteresis, large gradient values are required for droplet motion.) For hydrophobic surfaces, Figure 6b shows the required gradient value for spontaneous droplet motion on a surface where $R = 2$ mm and $\theta_{adv} = 120°$. Like before, the magnitude of the dr/dx value increases with both increasing r_o (i.e., increased initial roughness) and increasing contact angle hysteresis (i.e., $\theta_{adv} - \theta_{rec}$). It is also interesting to note when comparing Figure 6a and b that the absolute magnitude of dr/dx is always consistently larger for the hydrophilic surface than the hydrophobic surface as might be expected. In other words, achieving spontaneous droplet motion on a hydrophilic surface is more difficult than on a hydrophobic surface.

Surface Preparation. Microsized, parallel channels of variable width and a depth of 100 μm were laser-etched into a copper plate to form a test region 19.05 mm by 19.05 mm (0.75 in. by 0.75 in.) in size. The channel land had a fixed width of approximately 15 μm; however, the spacing between channels was varied gradually from 15 to 300 μm as shown in Figure 7. In this case, the initial roughness parameter r_o equaled 7.667, and the final roughness parameter r_{final} equaled 1.635.
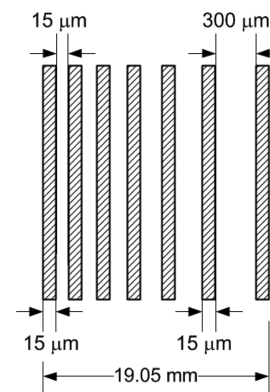
Figure 7. Surface tension gradient pattern (i.e., fixed land width, variable spacing).

Since the roughness parameter r was varied systematically along the surface, the dr/dx value for this surface is approximately -0.32 mm^{-1} as shown below where

$$dr/dx = (1.635 - 7.667)/19.05 \text{ mm} \qquad (16)$$

The etching was performed by a company in Dayton, OH using a 355 nm Nd:YVO4 laser system. Copper was chosen because it is naturally hydrophilic and is the material of choice in many heat and mass transfer applications. Prior to etching, the plates were first cleaned with acetone and isopropyl alcohol and dried using a stream of nitrogen gas. It is important to note however that *no* chemical modification of the surface was performed. A scanning electron microscopy (SEM) image of the final etched surface is shown in Figure 8.

Experimental Apparatus and Instrumentation. The apparent contact angles, base dimensions, and overall travel distances of droplets were obtained using a Ramé-Hart goniometer in combination with an overhead high-resolution CCD camera attached to a tripod. Droplets were placed on the surface using a high-precision microsyringe and photographed. Standard imaging software (KAPPA ImageBase) was then used to determine the exact initial droplet location on the gradient surface and the distance traveled with respect to a fixed edge using a before and after image of the droplet. Distance was determined by pixel counting and by initially calibrating against a known distance (i.e., standard). Both the front side and back side of a droplet were used to track the droplet's position on the gradient surface. Droplets 4–10 μL in size were examined. Typical uncertainty
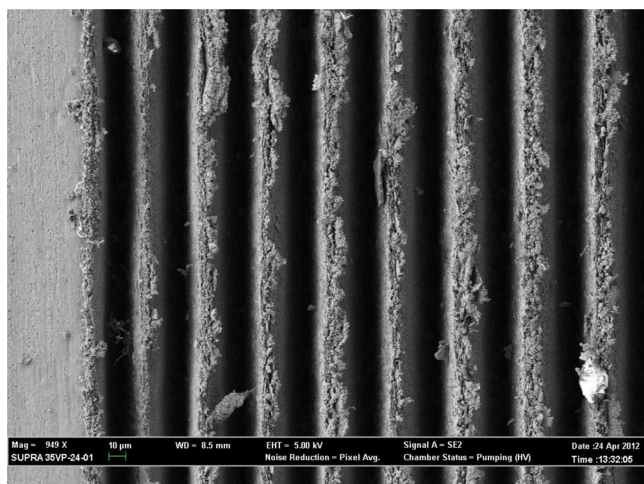
Figure 8. SEM image of the laser-etched microgrooved copper surface.

in the droplet travel distance was 5−6% with the maximum uncertainty not exceeding 12%, while the average uncertainty in the measured contact angle was 1°−2°.

■ RESULTS AND DISCUSSION

During experimentation, the laser-etched sample exhibited regions of clear hydrophobicity and regions of hydrophilicity. As designed and as expected, regions of narrow channel spacing were hydrophobic, and regions of wide channel spacing were hydrophilic. Perhaps more notably, droplets injected on the surface were observed to consistently follow the direction of the gradient as shown in Figure 9. Droplet movement was repeatable and spontaneous. A few other observations are worth mentioning. First, travel distances of 0.5−1.5 mm were measured (see Figure 10). Both the front and back of the droplet were observed to move; however, the front (or advancing) side of the droplet traveled on average slightly farther than the back (or receding) side of the droplet. In fact,
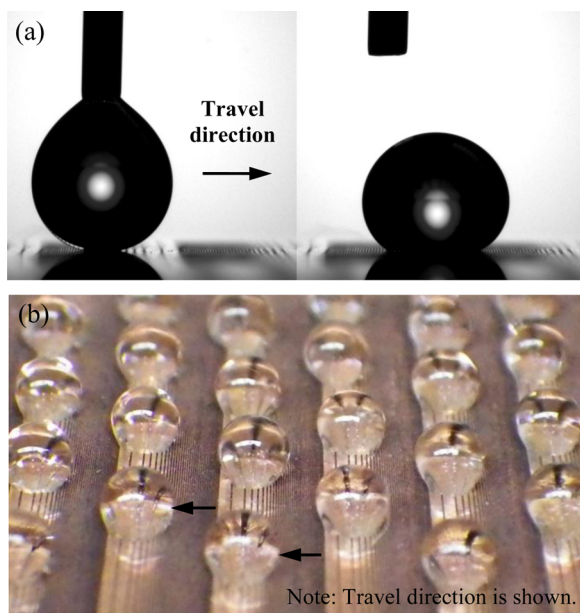
Figure 9. (a) Example of droplet movement with the gradient following injection on the surface. (b) Photograph illustrating the repeatability of this droplet motion.

in a few cases, droplet movement was only observed on the advancing side of the droplet. There was also no discernible correlation between the distance that the droplet traveled and its initial position on the gradient. In other words, the initial location of the droplet on the gradient did not play a significant role in the overall total distance traveled. This is likely because the droplets were all placed at nearly the same location on the surface.

Second, these measured distances agreed reasonably well with initial predictions made using the theoretical model presented in this work. Although it was not possible to accurately measure the advancing and receding angles on the laser-etched copper surface, one can infer approximate values from recorded images of droplets moving on the surface. (Note: Droplet movement was too rapid to permit accurate measurement of these angles. Moreover, on a gradient surface that is by nature nonhomogeneous, contact angles are location-dependent further complicating efforts to accurately measure their values.) Nonetheless, for θ_{adv} = 150° (estimated) and θ_{rec} = 130° (assumed) with R = 2 mm and r_o = 7.667 (as reported earlier) which represents the roughness parameter on the far side of the gradient, the predicted travel distance is 0.659 mm. If receding angles of θ_{rec} = 120° and 140° are used instead and the other parameters are held constant, the theoretical travel distances become 0.411 and 1.443 mm, respectively. Thus, considering the uncertainty in these values, reasonable agreement was observed.

Third, spontaneous droplet movement was observed on the $x−y$ plane (see Figure 2) in both horizontal and inclined surface orientations. Repeatable droplet movement was observed for surface inclination angles up to 5.7°; however, droplets were observed on occasion to move uphill for surface inclination angles up to 11°. (Note: For the purpose of this study, repeatable droplet movement was defined as a 90% or greater observation rate.) Fourth, it should be reemphasized that this spontaneous droplet motion was accomplished without the aid of surface chemistry modification. (That is, no chemical coating was used in this work.) Instead, it was solely accomplished by modifying the surface topography in such a way as to create a preferential wetting direction on the surface. This is particularly noteworthy since surface coatings can (and often do) wear off in application.

Qualitative tests were also performed to assess the ability of the surface tension gradient to direct water to prescribed drainage paths on the surface. For these tests, a laboratory squirt bottle was used to douse the lower portion of the surface (which contained the gradient) with water, and video (see the Supporting Information) was then recorded of the water's ensuing drainage characteristics. It was clear from these tests that the draining water followed clear paths along the surface which coincided with the hydrophilic end region of the gradient. As shown in Figure 11, the water drained readily along these paths as it sought to avoid contact with the hydrophobic region of the gradient. In fact, if the water was initially located near the top of the patterned surface, it would even move up and over one of these hydrophobic regions in order to drain down the preferred hydrophilic "gutter" region to the bottom of the surface. Again, it should be noted that this was accomplished without the aid of any chemical coating.

■ CONCLUSIONS

This paper presents a novel method for creating a topography-based surface tension gradient on a metallic surface for the
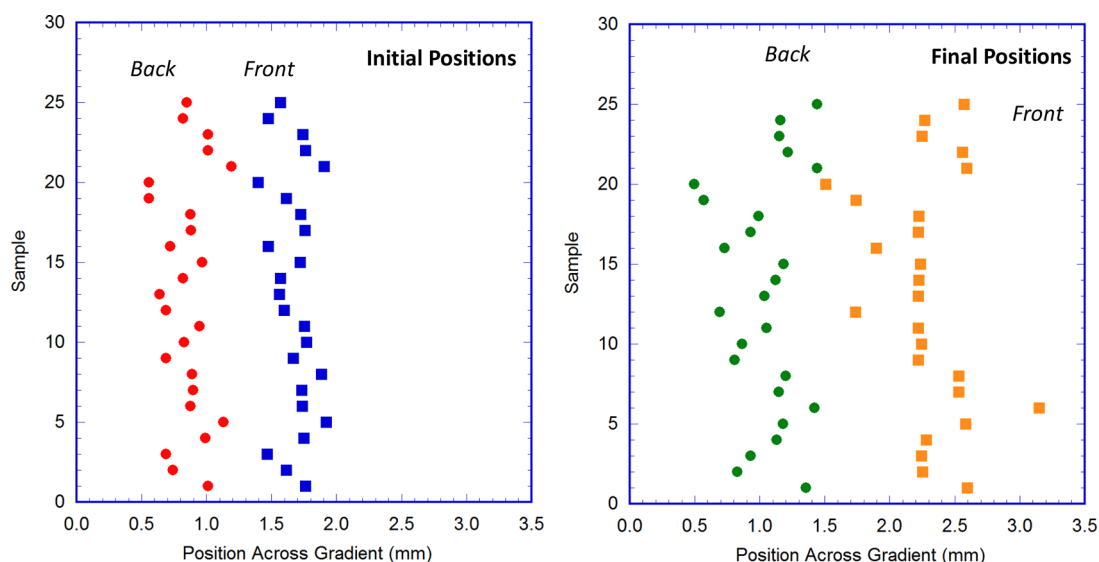
Figure 10. Droplet travel distances on the single gradient surface. Both the front and back side locations of the droplet are noted.
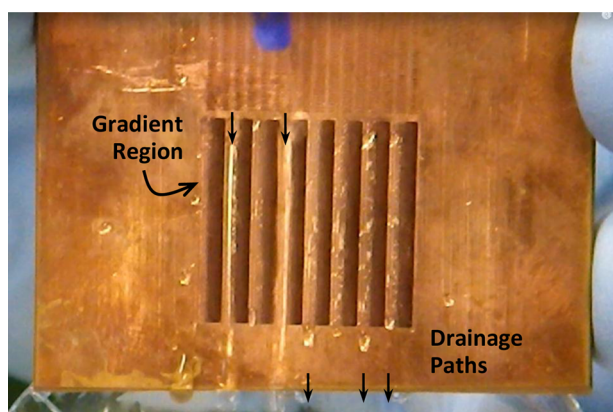
Figure 11. Water drainage behavior for the single gradient copper surface. The water was observed to consistently follow paths on the surface favored by the gradient. (Note: The laser etched regions appear dark in this image. A close-up view of these regions can be seen in Figure 9b.)

purpose of facilitating water droplet movement in preferred and prescribed directions along the surface. More specifically, in this work, parallel microchannels having a fixed land width but variable spacing were laser-etched into copper substrates to create a surface tension gradient on the surface. The surfaces were fabricated using a 355 nm Nd:YVO4 laser system and then characterized using spray testing techniques and water droplet (2−10 μL) injection via microsyringe. The distances that individual droplets traveled on the gradient surface were measured using a goniometer and CCD camera and found to be between 0.5 and 1.5 mm for the horizontal orientation. Droplet movement was spontaneous and did not require the use of chemical coatings.

A theoretical model was also presented which enables the minimum gradient (i.e., dr/dx) needed for spontaneous droplet movement on a horizontal surface to be calculated using Wenzel's model of wetting. The model which requires four inputs (i.e., droplet radius, advancing angle, receding angle, and surface roughness parameter) can be used to design and construct a topography-based surface tension gradient that utilizes parallel microchannels of variable spacing. The results of

this study suggest that microstructural patterning could be used to help reduce condensate retention on metallic fins such as those used in heat exchangers in HVAC&R applications.

■ ASSOCIATED CONTENT

Ⓢ Supporting Information
Video of water drainage behavior along prescribed drainage paths on the copper gradient surface shown in Figure 11. This material is available free of charge via the Internet at http://pubs.acs.org.

■ AUTHOR INFORMATION

Corresponding Author
*E-mail: sommerad@miamioh.edu. Phone: 513-529-0718. Fax: 513-529-0717.

Notes
The authors declare no competing financial interest.

■ ACKNOWLEDGMENTS

■ NOMENCLATURE

D	droplet diameter (mm)
F	force (mN)
g	acceleration due to gravity (m s^{-2})
k	retentive force factor (−)
m	droplet mass (mg)
r	roughness factor (−)
R	droplet radius (mm)
t	time (s)
V	droplet volume (μL)
w	channel width/spacing (μm)
x, y, z	coordinate axes

Greek Symbols

α	surface inclination angle (°)

δ channel depth (μm)
ϕ azimuthal angle (°)
γ surface tension (N m^{-1})
θ apparent contact angle (°)
ψ surface gradient parameter (mm^{-1})
ζ droplet base contour radius (mm)

Subscripts

adv   advancing
rec   receding
min   minimum
max   maximum
o   initial
s   surface tension

■ REFERENCES

(1) U.S. Energy Information Administration. *Annual Energy Outlook 2011 Early Release Report*, Report No: DOE/EIA-0383ER(2011); http://www.eia.doe.gov/forecasts/aeo/index.cfm, retrieved on 2011-02-21.

(2) Sommers, A. D.; Jacobi, A. M. Creating micro-scale surface topology to achieve anisotropic wettability on an aluminum surface. *J. Micromech. Microeng.* **2006**, *16* (8), 1571−1578.

(3) Chaudhury, M. K.; Whitesides, G. M. How to make water run uphill. *Science* **1992**, *256*, 1539−1541.

(4) Elwing, H.; et al. A wettability gradient method for studies of macromolecular interactions at the liquid-solid interface. *J. Colloid Interface Sci.* **1986**, *119*, 203−210.

(5) Daniel, S.; Chaudhury, M. K.; Chen, J. C. Fast drop movements resulting from the phase change on a gradient surface. *Science* **2001**, *291*, 633−636.

(6) Daniel, S.; Chaudhury, M. Rectified motion of liquid drops on gradient surfaces induced by vibration. *Langmuir* **2002**, *18*, 3404−3407.

(7) Shastry, A.; Case, M. J.; Böhringer, K. F. Directing droplets using microstructured surfaces. *Langmuir* **2006**, *22* (14), 6161−6167.

(8) Daniel, S.; et al. Ratcheting motion of liquid drops on gradient surfaces. *Langmuir* **2004**, *20*, 4085−4092.

(9) Moumen, N.; Subramanian, R. S.; McLaughlin, J. B. Experiments on the motion of drops on a horizontal solid surface due to a wettability gradient. *Langmuir* **2006**, *22*, 2682−2690.

(10) Moradi, N.; Varnik; Steinbach, I. Roughness-gradient-induced spontaneous motion of droplets on hydrophobic surfaces: A lattice Boltzmann study. *EPL* **2010**, *89*, No. 26006.

(11) Blanchette, F.; Messio, L.; Bush, J. W. M. The influence of surface tension gradients on drop coalescence. *Phys. Fluids* **2009**, *21*, No. 072107.

(12) Darhuber, A. A.; Valentino, J. P.; Troian, S. M.; Wagner, S. Thermocapillary actuation of droplets on chemically patterned surfaces by programmable microheater arrays. *J. Microelectromech. Syst.* **2003**, *12* (6), 873−879.

(13) Zhu, X.; Wang, H.; Liao, Q.; Ding, Y. D.; Gu, Y. B. Experiments and analysis on self-motion behaviors of liquid droplets on gradient surfaces. *Exp. Therm. Fluid Sci.* **2009**, *33*, 947−954.

(14) Zhang, J.; Han, Y. Shape-gradient composite surfaces: Water droplets move uphill. *Langmuir* **2007**, *23*, 6136−6141.

(15) Hong, D.; Cho, W. K.; Kong, B.; Choi, I. S. Water-collecting capability of radial-wettability gradient surfaces generated by controlled surface reactions. *Langmuir* **2010**, *26* (19), 15080−15083.

(16) Bliznyuk, O.; Jansen, H. P.; Kooij, E. S.; Zandvliet, H. J. W.; Poelsema, B. Smart design of stripe-patterned gradient surfaces to control droplet motion. *Langmuir* **2011**, *27*, 11238−11245.

(17) Cheng, J.; Zhang, Y.; Pi, P.; Lu, L.; Tang, Y. Effect of gradient wetting surface on liquid flow in rectangular microchannels driven by capillary force and gravity: An analytical study. *Int. Commun. Heat Mass Transfer* **2011**, *38*, 1340−1343.

(18) Wu, J.; Ma, R.; Wang, Z.; Yao, S. Do droplets always move following the wettability gradient? *Appl. Phys. Lett.* **2011**, *98*, 204104.

(19) Fang, G.; Li, W.; Wang, X.; Qiao, G. Droplet motion on designed microtextured superhydrophobic surfaces with tunable wettability. *Langmuir* **2008**, *24* (20), 11651−11660.

(20) Luo, M.; Gupta, R.; Frechette, J. Modulating contact angle hysteresis to direct fluid droplets along a homogeneous surface. *ACS Appl. Mater. Interfaces* **2012**, *4*, 890−896.

(21) Langley, K. R.; Sharp, J. S. Microtextured surfaces with gradient wetting properties. *Langmuir* **2010**, *26* (23), 18349−18356.

(22) Genzer, J.; Bhat, R. R. Surface-bound soft matter gradients. *Langmuir* **2008**, *24* (6), 2294−2317.

(23) Khoo, H. S.; Tseng, F.-G. Spontaneous high-speed transport of subnanoliter water droplet on gradient nanotextured surfaces. *Appl. Phys. Lett.* **2009**, *95*, 063108.

(24) El Sherbini, A. I. Modeling Condensate Drops Retained on the Air-Side of Heat Exchangers. Ph.D. Thesis, University of Illinois at Urbana-Champaign, Urbana, IL, 2003.

(25) Dussan V., E. B.; Chow, R. T.-P. On the Ability of Drops or Bubbles to Stick to Non-Horizontal Surfaces of Solids. *J. Fluid Mech.* **1983**, *137*, 1−29.

(26) Extrand, C. W.; Gent, A. N. Retention of Liquid Drops by Solid Surfaces. *J. Colloid Interface Sci.* **1990**, *138*, 431−442.

(27) Extrand, C. W.; Kumagai, Y. Liquid Drops on an Inclined Plane: The Relation Between Contact Angles, Drop Shape, and Retentive Force. *J. Colloid Interface Sci.* **1995**, *170*, 515−521.

(28) Wenzel, T. N. Resistance of solid surfaces to wetting by water. *Ind. Chem. Eng.* **1936**, *28* (8), 988−994.

(29) Dimitrakopoulos, P.; Higdon, J. J. L. On the Displacement of Three-Dimensional Fluid Droplets Adhering to a Plane Wall in Viscous Pressure-Driven Flows. *J. Fluid Mech.* **2001**, *435*, 327−350.

(30) Öner, D.; McCarthy, T. J. Ultrahydrophobic surfaces: effects of topography length scales on wettability. *Langmuir* **2000**, *16*, 7777−7782.

(31) Chen, W.; Fadeev, A. Y.; Hsieh, M. C.; Öner, D.; Youngblood, J.; McCarthy, T. J. Ultrahydrophobic and ultralyophobic surfaces: some comments and examples. *Langmuir* **1995**, *15*, 3395−3399.

(32) Jopp, J.; Grüll, H.; Yerushalmi-Rozen, R. Wetting behavior of water droplets on hydrophobic microtextures of comparable size. *Langmuir* **2004**, *20*, 10015−10019.

(33) Furstner, R.; Barthlott, W.; Neinhuis, C.; Walzel, P. Wetting and self-cleaning properties of artificial superhydrophobic surfaces. *Langmuir* **2005**, *21*, 956−961.